Geological Quarterly, 2024, 68, 36
DOI: http://dx.doi.org/10.7306/gq.1764

EMPA U-Th-total Pb dating of uraninite from the Stara Kamienica schist belt (West Sudetes, SW Poland): new data towards interpreting the genesis of cassiterite-sulphide mineralization

Rafał MAŁEK[1, *] and Stanisław Z. MIKULSKI[2]

[1] Multiconsult Polska sp. z o.o., Bonifraterska 17, 00-203 Warszawa, Poland; ORCID: 0000-0003-3163-2433

[2] Polish Geological Institute – National Research Institute, Rakowiecka 4, 00-975 Warszawa, Poland; ORCID: 0000-0002-9941-5630

Małek, R., Mikulski, S.Z., 2024. EMPA U-Th-total Pb dating of uraninite from the Stara Kamienica schist belt (West Sudetes, SW Poland): new data towards interpreting the genesis of cassiterite-sulphide mineralization. Geological Quarterly, 68, 36; https://doi.org/10.7306/gq.1764

Associate editor: Tomasz Bajda

Electron microprobe analyses of mineral samples from archival drilling cores from the Stara Kamienica schist belt, Western Sudetes, were applied to help interpret cassiterite-sulphide mineralization known for centuries, but still of unclear origin. The new data, including EMPA U-Th-total Pb dating of uraninites coeval with cassiterite-sulphide mineralization, help inform discussion of the genesis of this tin mineralization. The uraninites analyzed, scattered within micas in the schists, have homogeneous internal structure without any cracks and clear grain edges, which may indicate their hydrothermal origin. Results of uraninite dating indicate two age ranges: approximately 300–310 and 345–360 Ma, which may suggest crystallization of the cassiterite-sulphide mineralization during hydrothermal metasomatic processes related, respectively, to regional metamorphism and the final emplacement of the Karkonosze granitoid intrusion.

Key words: EMPA, U-Th-total Pb dating, uraninite, Stara Kamienica, Sudetes.

INTRODUCTION

Stara Kamienica schist belt in the West Sudetes, Poland, part of the Karkonosze-Izera metamorphic unit, is built mainly of quartz-chlorite-mica schist within which cassiterite with accompanying sulphide mineralization has been recognized (Michniewicz et al., 2006). The study area saw tin ore mining activity from the beginning of 16th century, while in the middle of 20th century two deposits of tin ore (Krobica and Gierczyn) were documented within it and a number of prospective areas were noted (e.g., Krobica Zachód – Czerniawa and Przecznica; Małek et al., 2019, with references therein).

Discussions continue about the genesis and source of mineralization contained in the Stara Kamienica schist belt. Electron microprobe analysis (EMPA) U-Th-total Pb dating of accessory uraninites, occurring in association with ore minerals, has the potential to provide new data. U-Pb dating (Parrish, 1990) by EMPA can precisely date monazite [(Ce,La,Nd,Th)PO_4] (e.g., Suzuki and Adachi, 1991a, b; Montel et al., 1996; Cocherie et al., 1998) and also uraninite [UO_2], and xenotime [YPO_4] (e.g., Cross et al., 2011; Ozha et al., 2017; Griffin et al., 2020).

The age is determined by measuring U, Th, and Pb, assuming that there is negligible common lead, that the isotopes of U are present in their crustal abundances, and that elemental concentrations have not been significantly modified by subsequent mass transfer (Montel et al., 1996; Cocherie et al., 1998). This method determines the approximate age of a given grain based on a mathematical calculation involving the UO_2, ThO_2 and PbO content ratios (in weight %) measured with a Cameca SX-100 electron microprobe (Kusiak, 2007). Radiogenic Pb accumulates in uraninite and other minerals with significant Th and/or U (e.g., thorite, monazite, xenotime).

The analysis of Th, U, and Pb in monazite by EMPA involves two equally critical aspects: (a) obtaining adequate precision (sufficient counts) to achieve acceptable detection limits and errors relative to the questions being asked and (b) obtaining accurate concentrations. The first point is primarily a function of counting parameters (intensity, total acquisition time per point, and total number of points in the analysis). The second point is far more difficult to evaluate and is a function of many possible analytical effects (Jercinovic and Williams, 2005; Pyle et al., 2005; Williams et al., 2007).

EMPA dating consists of analysing multiple spots within homogeneous age domains that show sufficient compositional variation, and then these data are used to construct a *"pseudo-*

---

* Corresponding author, e-mail: rafal.malek@multiconsultgroup.com

Received: June 18, 2023; accepted: September 11, 2024; first published online: November 12, 2024

isochron" from which an age can be obtained *via* regression. This method has the potential advantage of adequate precision, and the ability to work with minerals that have a significant initial common Pb component. This technique can identify two or more homogeneous domains that are separated by age gaps smaller than the error on individual spot age analyses (Suzuki and Kato, 2008). EMPA dating method can produce accurate and moderately precise ages of mineral growth. It has the advantages of being non-destructive, of high spatial resolution, achievable with widely available electron microprobe instruments, and is workable on minerals with less-radiogenic (or initial) Pb contents (Suzuki and Dunkley, 2015).

The aim of using EMPA U-Th-total Pb dating method was to determine the age of accessory uraninite within the Stara Kamienica mica schist. The uranium mineralization within the northern cover of the Karkonosze Granite, including schists of the Stara Kamienica belt, has been studied by many researchers. Most of them attribute the formation of the uranium minerals to metasomatic and hydrothermal activity related to granite intrusions and regional metamorphism (e.g., Mochnacka and Banaś, 2000 with references therein). Any new data related to the ages of hydrothermal uranium minerals from this area could help determine the origin, processes and geological history of the cassiterite-sulphide mineralization within the Stara Kamienica schist belt.

GEOLOGICAL SETTING

The West Sudetes constitute the northernmost, exposed region of the Bohemian Massif's Saxothuringian zone (Franke and Żelaźniewicz, 2000; Konopásek et al., 2019). The southern part of the Western Sudetes is the Karkonosze-Izera Massif, the core of which is a granitoid complex (the protolith is early Paleozoic in age, Borkowska et al., 1980; Kröner et al., 2001) surrounded by metamorphosed sedimentary and volcanic rocks (Kryza et al., 1995, 2007; Winchester et al., 1995, 2003; Žáčková et al., 2012). The geotectonic development of the area began with the subduction of the Saxothuringian Ocean, accompanied by the development of high-pressure mineral associations within both mafic and felsite rocks (Kryza et al., 1990; Smulikowski, 1995; Žáčková et al., 2010; Majka et al., 2016). The later stages of the region's evolution consist of the uplift of high-pressure subduction rocks, their extensive retrogression in greenschist facies conditions, and post-metamorphic folding of the rocks of the entire complex. Subsequently, around 320–312 Ma, the Karkonosze plutonic complex intruded into the Karkonosze-Izera massif (Machowiak and Armstrong, 2007; Kryza et al., 2014; Mikulski et al., 2020).

The Karkonosze granitoid intrusion, stretching for ~70 km in an E–W direction, is the central part of the Karkonosze-Izera metamorphic unit, which separates the metamorphic formations into two units: the Izera metamorphic unit (northern cover of the Karkonosze granite) and the eastern-southern Karkonosze metamorphic unit (Smulikowski, 1972). The Izera Metamorphic unit consists of two main rock complexes. The first of these, predominating in terms of area, comprises the the pre-Variscan Izera granites, gneisses and granite-gneisses. The second complex consists of lithologically diverse schists, whose dominant components are quartz, micas and chlorites with variable quantitative relations. Within the gneiss-granitoid complex, the schists form five relatively narrow, E–W-aligned belts (Fig. 1; Oberc, 1961; Michniewicz et al., 2006). From south to north they are: the Szklarska Poręba schist belt, the Stara Kamienica schist belt, the Mirsk schist belt, the Jindřichovice schist belt and the Złotniki Lubańskie schist belt.

The origin of the schist bodies of the Izera Metamorphic unit is considered to be the result of supracrustal metamorphism (Oberc, 1961; Oberc-Dziedzic, 1975), while in the case of the gneiss-granite complex, there are three main ideas regarding its origin. The first of these suggests a metamorphosed and transformed set of infracrustal rocks (Borkowska et al., 1980), the second one focuses on the granitization of the supracrustal rocks, resulting in the transition from schist through gneisses and granitogneisses to granitoid rocks (Oberc, 1961, 1972; Oberc-Dziedzic, 1975). The third view interprets the genesis as from coexistence of both developmental sequences described above, with homogenization locally causing the blurring of original differences between the supra- and intra-crustal rocks (Kozłowska-Koch, 1965; Smulikowski, 1972; Kozłowski, 1974; Żaba, 1984; Oberc-Dziedzic, 1988; Mazur and Aleksandrowski, 2001).

It is inferred that the schist complex of the Karkonosze-Izera massif is of Precambrian age, this inference being based on a number of observations and geological premises (Michniewicz et al., 2006). Rb-Sr dating of the Izera gneiss-granitoid complex and also U-Pb and Pb-Pb dating of zircons indicates an age range of 452–501 Ma, i.e the Late Cambrian–Late Ordovician stratigraphic interval (Borkowska et al., 1980, Oliver et al., 1993; Korytowski et al., 1993; Kröner et al., 1994).

The Stara Kamienica schists are fine-grained rocks with a granolepidoblastic structure, light grey or silvery grey in colour (often with a greenish tint), with clearly marked foliation and lamination (Fig. 2). Their main mineral components are muscovite and quartz, which are present in all lithological varieties recognized. Chlorite and biotite occur less frequently and may occur together or interchangeably. Within this rock complex there are levels with chloritoid and garnets, which often can play a significant role in the mineral composition of the schists. A number of schist accessory minerals have been recognized, including albite, staurolite, gahnite, margarite, apatite, tourmaline, zircon, monazite, xenotime, ilmenite and others (Michniewicz et al., 2006, with references therein). Throughout the whole schist succession, regardless of the lithological variety and mineral proportions, lenses, boudins and quartz folds are observed. Lamination in the schists is made of alternating quartz- and mica-rich layers.

THE CASSITERITE-SULPHIDE MINERALIZATION

The main tin mineral of the Stara Kamienica schists is cassiterite (SnO_2), that forms grains <0.1 mm across (i.e. Harańczyk and Skiba, 1961; Kowalski et al., 1978; Wiszniewska, 1984; Bobiński, 1997; Michniewicz at al., 2006; Mikulski et al., 2018; Małek et al., 2019). It occurs as single grains or larger clusters in association mainly with quartz and chlorite, and slightly less frequently with sulphides, muscovite, chloritoid and biotite (Fig. 3). Cassiterite occurs in the schists in two varieties, brown and colourless, usually forming aggregates, lamellar or irregular clusters and also as single crystals. Grain clusters of cassiterite are arranged parallel to the foliation of the schists, forming pseudo-laminae and lenses. (Siemiątkowski, 1991; Michniewicz et al., 2006, with references therein). The cassiterite is accompanied by ore minerals: mainly sulphides, but also oxides, sulphur salts, arsenides and native metals (e.g., native bismuth; Małek, 2022). The most common forms of sulphide occurrence are layers consistent with the rock foliation (thickness up to several mm), pseudo-layers composed of speckled accumulations, massive clusters, impregnations emphasizing the schist foliation and fine veins transverse to it. In total, over 50 ore minerals have been recognized; most

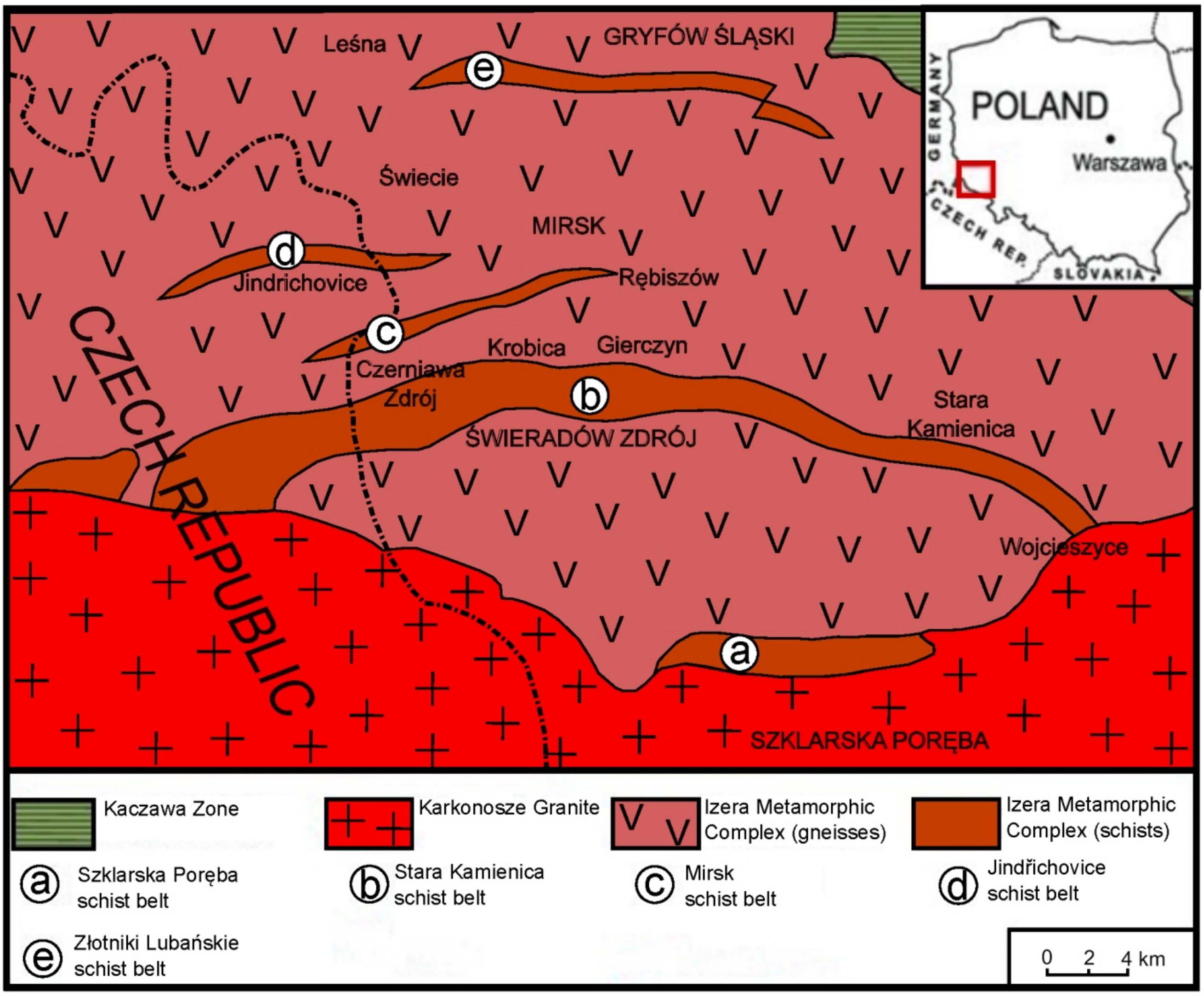

Fig. 1. Schist belts within the Izera Metamorphic Complex (after Michniewicz et al., 2006, modified)

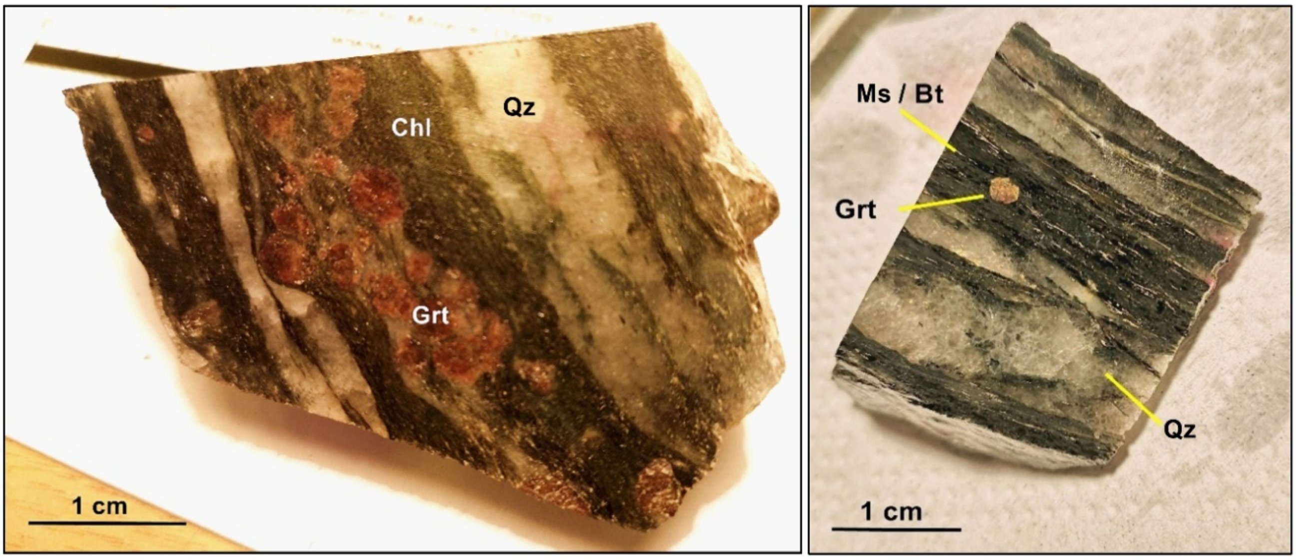

Fig. 2. Macroscopic view of the Stara Kamienica schists: chlorite (Chl) – biotite (Bt) – muscovite (Ms) – quartz (Qz) schists with accessory garnet (Grt)

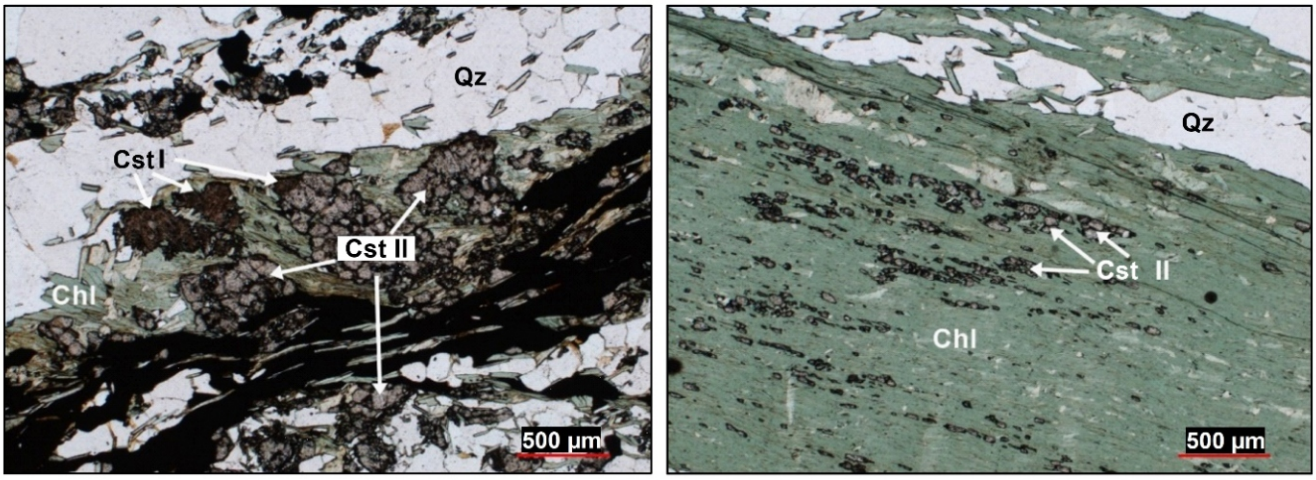

Fig. 3. Optical microscope images of the Stara Kamienica schists with the characteristic cassiterite mineralization

Left – brown cassiterite (older, Cst I) replaced by colourless cassiterite (younger, Cst II) within chlorite (Chl) – quartz (Qz) schists; right – cassiterite (Cst II) within a chlorite lamina

of them occur sporadically in small amounts and are of only academic significance. The dominant ore minerals recognized within the schists along the entire width examined of the Stara Kamienica belt are pyrrhotite, chalcopyrite, pyrite, arsenopyrite, sphalerite, galena, ilmenite, bismuthinite as well as native bismuth. The observations of many researchers indicate that the sulphide and ore mineralization superimposed on pre-existing cassiterite mineralization, but it is impossible to distinguish clear genetic connections between the cassiterite and sulphide mineralization, which do not always coexist (Michniewicz et al., 2006, with references therein).

Researchers do not agree on the origin of cassiterite-sulphide mineralization in the Stara Kamienica schists. We can currently distinguish four distinct groups of views on the origin of the mineralization, each with their own arguments. The first is in favour of a syngenetic, sedimentary genesis of the cassiterite-sulphide mineralization, which underwent later metamorphism (i.e. Jaskólski, 1960, 1963; Szałamacha, 1967, 1976). The second group of views speaks of a pre-metamorphic (pre-Variscan) hydrothermal genesis related to an originally igneous complex of the Izera gneisses (i.e., Harańczyk and Skiba, 1961; Siemiątkowski, 1986, 1988, 1989; Michniewicz, 1988, 1996; Cook and Dudek, 1994; Bobiński, 1997; Michniewicz et al., 2006). The third theory presents arguments for the hydrothermal, post-metamorphic genesis of the mineralization, which is temporally and spatially related to the Variscan intrusion of the Karkonosze granitoid (i.e., Jaskólski and Mochnacka, 1959; Kowalski et al., 1978; Kozłowski, 1978; Karwowski and Włodyka, 1981; Wiszniewska, 1983, 1984; Speczik and Wiszniewska, 1984; Berendsen et al., 1987; Piestrzyński et al., 1992; Kucha and Mochnacka, 1998). Fourthly, Mikulski et al. (2007), in relation to the As mineralization at Czarnów, which is part of the eastern cover of the Karkonosze granite, built of analogous schists containing cassiterite and sulphide mineralization, proposed a much more complex metasomatic-hydrothermal genesis associated with multi-stage development of intrusive-metamorphic processes of pre-Variscan and Variscan ages.

MATERIALS AND METHODS

Samples were selected from archival drilling cores from the Stara Kamienica schist belt, the historic St. Johannes and St. Leopold mines in Krobica, a mica schist quarry in Orłowice and post-mining heaps in Gierczyn (Mikulski et al., 2018).

Back-scattered electron (BSE) imaging and compositional analyses were carried out on carbon-coated thin sections using a *CAMECA SX-100* X-ray microprobe in the Micro-area Analyses Laboratory at the Polish Geological Institute – National Research Institute (Warszawa, Poland). Detailed observations and analyses of chemical composition using WDS (wavelength dispersive spectroscopy) detectors were focused on a number of uraninite grains. The analytical conditions of the quantitative analyses of the uraninite studied were as follows: accelerating voltage of 15 or 20 kV, beam current of 10, 20 or 40 nA, focused beam diameter <1 µm and acquisition time at peak position of 20 s and in background position of 10 s.

The following parameters were used for the U-Th-total Pb dating: accelerating voltage 15 kV, current intensity in the first column 40 nA, and in the second column 200 nA, while the following analytical lines were used for the readings: Um , ThM , PbM . To calibrate the analysis, a xenotime standard from Iveland [Nor] was used with an U-Pb or Th-Pb age of 900 ± 52 Ma. Mathematical calculations were performed using the EMPA U-Th-total Pb dating software including the Age Map conversion program included in the PEAK SIGHT package. Full details of the EMPA analytical conditions are provided in Appendix 1.

RESULTS

Uraninite grains were recognized in two samples taken from the archival drilling cores from Krobica (borehole K-II/3, sample depth 250.6 m) and Gierczyn (borehole G-1/13, sample depth 154.9 m) sited in the central part of the Stara Kamienica schist

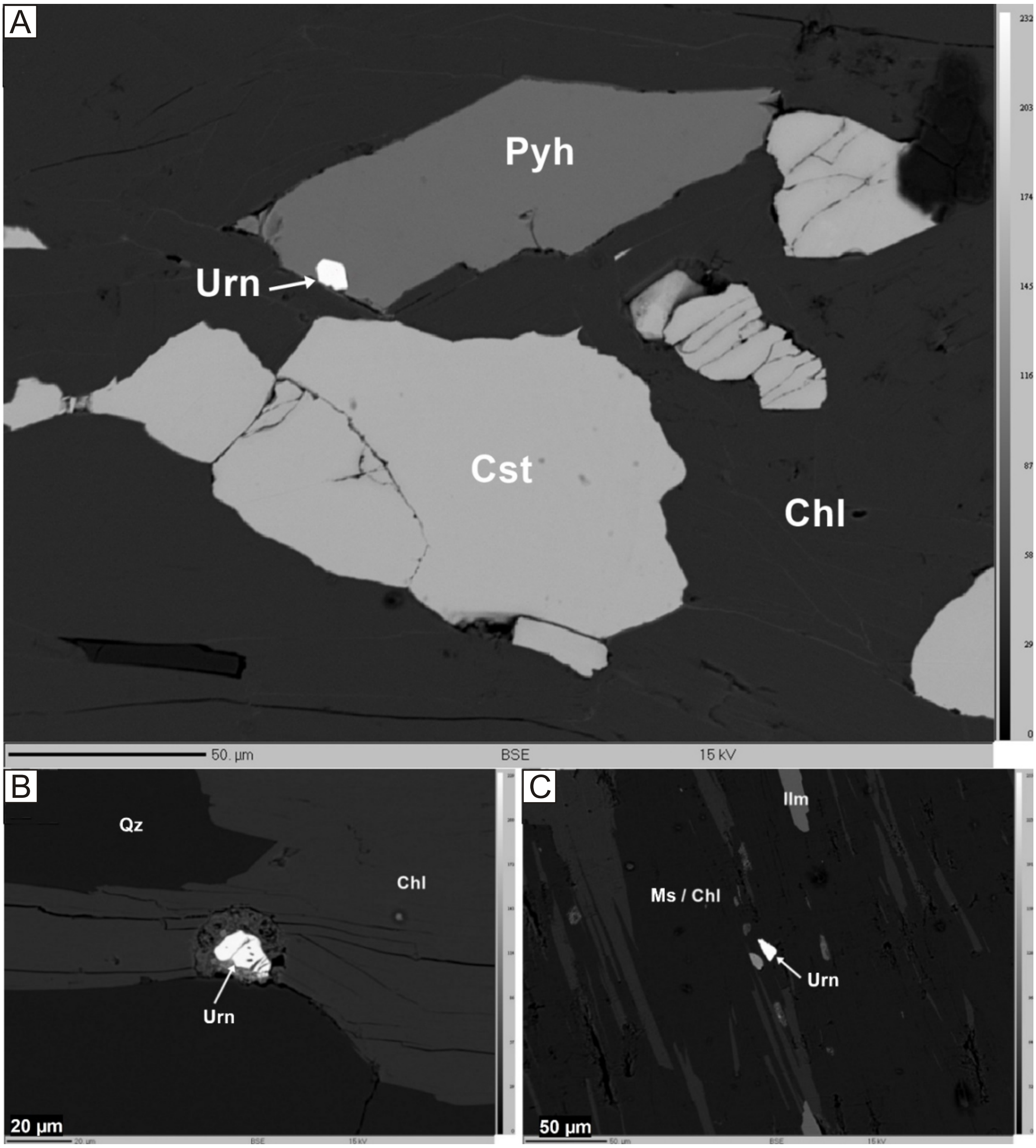

Fig. 4A – uraninite (Urn) intergrown with pyrrhotite (Pyh) in association with cassiterite (Cst) within a chlorite (Chl) lamina, Krobica K-II/3 borehole, BSEI (back-scattered electron image); B – cracked uraninite grain in chlorite-quartz (Qz) schist, Gierczyn G-I/13 borehole, BSE; C – common occurrence of uraninite in a muscovite-chlorite (Ms/Chl) lamina, Gierczyn G-I/13 borehole, BSE

belt (Fig.1). Uraninite in these occurs as an accessory mineral, observed in the form of small (usually up to 20 µm across), rounded xenomorphic grains, most often as inclusions in chlorite, but also in ore minerals such as pyrrhotite, pyrite and chalcopyrite (Fig. 4A). The uraninite grains analysed were characterized by a homogeneous internal structure and clear edges (Fig. 4C), which may indicate their hydrothermal origin. Occasionally, uraninite grains with small cracks and signs of metasomatic alternation were also found (Fig. 4B). The analyses of those grains showed higher measurement errors, and for that reason they were excluded from further consideration.

A total of 11 WDS analyses of the chemical composition of those uraninites (Table 1) whose grain shape and form of occurrence could indicate a hydrothermal origin were considered as suitable for calculating a U-Th-total Pb age. The average content of UO_2 in the uraninites analysed was 88.72 wt.%, the most significant admixtures being PbO (avg. 4.168 wt.%), FeO (avg. 1.518 wt.%), ThO_2 (avg. 0.396 wt.%) and Y_2O_3 (avg. 0.327 wt.%). Other oxides identified showed a measured average content of <0.3 wt.%. All compositional data of the EMPA analyses together with calculated U-Th-total Pb ages are provided in Appendix 2.

Table 1

U-Th-total Pb dating results of the uraninites

No.	Borehole / sample	Age [Ma]	Error ± Ma (1)
1	Kobica K-II/3	299	7
2	Kobica K-II/3	367	8
3	Kobica K-II/3	307	7
4	Kobica K-II/3	299	7
5	Kobica K-II/3	363	8
6	Kobica K-II/3	365	8
7	Kobica K-II/3	362	8
8	Gierczyn G-I/13	350	15
9	Kobica K-II/3	351	15
10	Kobica K-II/3	349	15
11	Kobica K-II/3	350	15

The micro-area analyses and the low measurement errors obtained (Table 1 and Appendix 2) mean that the dating of uraninites can be considered as reliable. The uraninite U-Th-total Pb ages obtained are clustered in two ranges: approximately 300–310 (3 results) and 345–360 Ma (8 results; Fig. 5). The geometric mean of the uraninite ages are as follows: 301.6 ±7 Ma (n = 3), 348.6 ±12.5 Ma (n = 4) and 362 ±8 Ma (n = 4).

DISCUSSION

The petrographic character of the uraninites studied may indicate their hydrothermal origin. Given the lack of more specific isotopic data, though, especially of common Pb in the uraninites, their hydrothermal origin is not certain. We assume that the crystallization ages obtained for these minerals correspond to hydrothermal events that led to both the uraninite and the cassiterite-sulphide mineralization, as their relationship was established by mineralogical and geochemical studies: observations of mineral paragenesis and co-occurrence of ore minerals with REE carrier minerals, the presence of uranium admixtures in the ore minerals and a positive correlation of uranium with some metals (e.g. Cu, Sn, Ag, In, Sb, W, and Bi: Małek, 2022). The dates obtained may allow reinterpretation of the origin of the cassiterite-sulphide mineralization in the Stara Kamienica schist belt.

Microprobe U-Th-total Pb dating of uraninites has been widely used for many years, particularly for dating hydrothermal events. An example of such an application was provided by Pieczonka et al. (2019), who, based on the PbO and REE contents in uraninite, distinguished two generations corresponding to separate hydrothermal events. Analyses of the chemical composition of uraninites from the Stara Kamienica schists do not show significant differences in Pb and REE content (PbO content in the range of 3.43–4.50 wt.%; for comparison Pieczonka et al. (2019) recorded PbO contents in uraninite ranging from 0.54 to 6.80 wt.%). Despite the lack of a varied chemical composition, of different forms of occurrence, or of relationships with other minerals, the uraninites from the Stara Kamienica schists were probably formed as a result of at least two hydrothermal events, as indicated by the results of the dates obtained.

The age of the Izera granite-gneiss complex is 452–501 Ma (Borkowska et al., 1980; Oliver et al., 1993; Korytowski et al., 1993; Kröner et al., 1994), much older than the mineral ages obtained in this study. The rocks of the Izera complex (specifically the granitoid protolith of the Izera rocks) cannot therefore be a source of hydrothermal solutions for the cassiterite-sulphide mineralization. The situation is slightly different in the case of the Karkonosze granitoid, where dating of individual lithological units indicate its formation in the range of ~300–330 Ma (Mikulski et al., 2020, with references therein). The uraninite age range of 301.6 ±7 Ma obtained in this study falls within the age range of the formation of the Karkonosze granite. The groups of uraninite dating results of 348.6 ±12.5 Ma and 362 ±8 Ma may indicate strong hydrothermal metasomatic processes related to regional metamorphism. This age is consistent with the Variscan orogeny, responsible for the metamorphism and deformation of the Izera area. It is probable that plutonic processes preceding the crystallization of the Karkonosze granite led to a series of hydrothermal events that contributed to the development of the metamorphic Izera area and the precipitation of cassiterite and other ore minerals within the Stara Kamienica schists, a geochemically different medium within the Izera granite complex. Recent studies of the Przecznica polymetallic mineralization, especially of lead isotopes using a Nu Plasma HR multicollector ICPMS with a laser ablation system (LA MC-ICP-MS) on galena, yielded crystallization ages of this mineral of ~694–744 Ma. Pb-Pb ages were

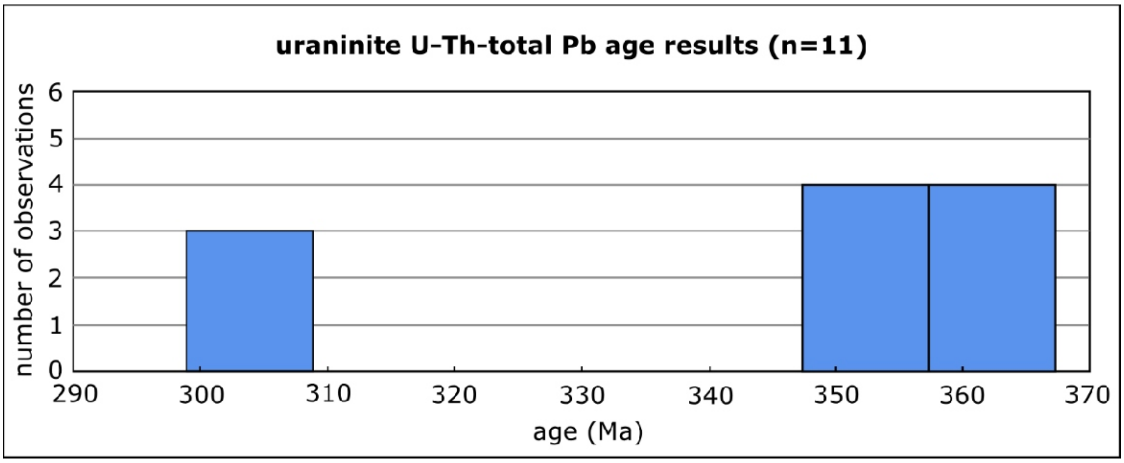

Fig. 5. Frequency histogram of the uraninite U-Th-total Pb dates

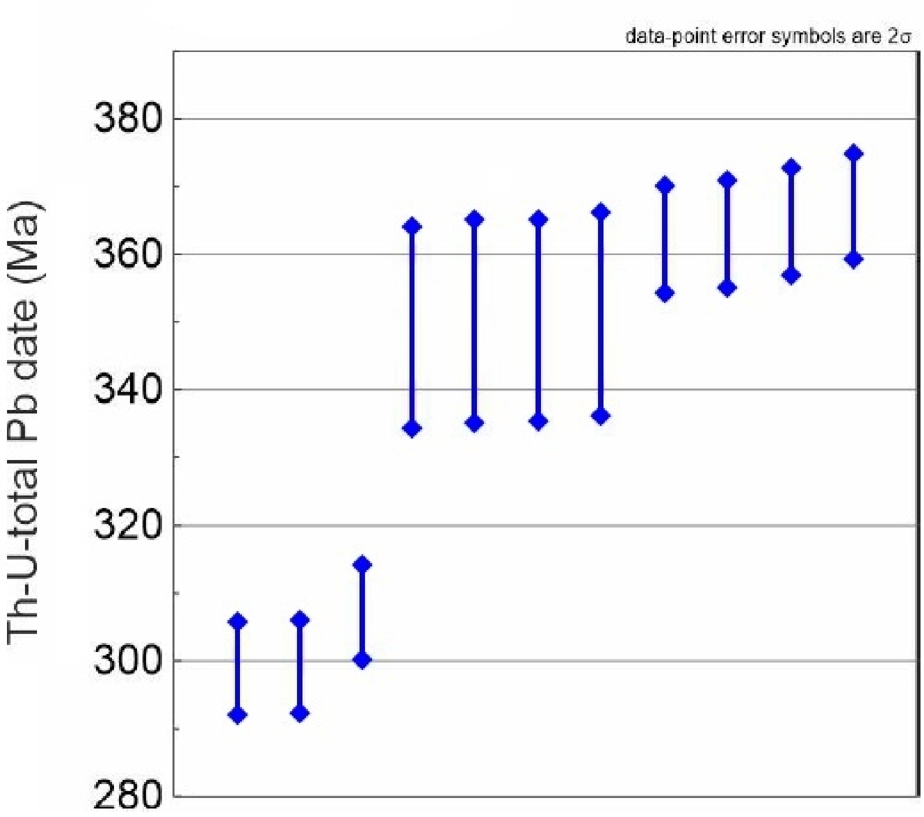

Fig. 6. Plot of the uraninite U-Th-total Pb dates obtained

calculated with PbIso (Armistead et al., 2021) using model parameters from Stacey and Kramers (1975) and gave Neoproterozoic ages. This may stand for a pre-Variscan age (and source of lead) for at least part of the Stara Kamienica schist mineralization (Foltyn et al., 2023). On the other hand, the results of LA-ICP-MS dating of cassiterites from the Gierczyn-Przecznica area provided by Zygo et al. (2023) seem to clearly correspond with EMPA U-Th-total Pb dating of uraninites revealed in this study. Those authors determined the ages of cassiterites as 353 ±14, 360 ±5 and 318 ±6 Ma. They inferred that the first event (353 ±14 and 360 ±5 Ma) may be related to the regional metamorphism while the second one (younger, 318 ±6 Ma) may be associated with the emplacement of the Karkonosze Granite.

We regard our chemical U-Th-total Pb age determination for the Stara Kamienica schist belt uraninite as possessing a lower level of confidence than the recent LA-ICP-MS dating results (e.g., Foltyn et al., 2023; Zygo et al., 2023). Without any control of the common Pb content of the Stara Kamienica schist belt uraninite grains studied, our EMPA chemical U-Th-total Pb age is best interpreted as a reconnaissance-level age determination as a prelude to more specific isotopic studies. However, the uraninite age results obtained with the EMPA U-Th-total Pb method correspond with the ages obtained by other authors, especially with the LA-ICP-MS cassiterite ages provided by Zygo et al., (2023).

Therefore, we conclude that the cassiterite-sulphide mineralization of the Stara Kamienica schists probably arose as a result of hydrothermal-metasomatic activity associated with the multi-stage development of intrusive and metamorphic processes of the Pre-Variscan and Variscan cycles leading to the formation of the Karkonosze granite and the evolution of the Izera massif. The U-Pb EMPA ages obtained of the hydrothermal uraninites, of approximately 348.6 ±12.5 Ma and 362 ±8 Ma, can be considered as a sign of regional metamorphism and hydrothermal activity while the younger age of 301.6 ±7 Ma may indicate later-stage hydrothermal processes associated with the Karkonosze granite intrusion. Similar conclusions, of complex, multi-stage genesis of polymetallic mineralization in the Czarnów area, occurring in analogous schists in the eastern part of the Karkonosze granitoid cover, were described by Mikulski et al. (2007).

Acknowledgements. This article is part of Rafał Małek's doctoral dissertation titled "Mineralogical-geochemical study and genesis of a rare and accompanying elements occurrence within the tin-bearing deposit mineralization of the Stara Kamienica schist belt in the Sudetes" under the supervision of Prof. Stanisław Z. Mikulski. Part of this work was financially supported by the Polish Geological Institute-National Research Institute through an internal grant no. 62.9012.2204.00.0.

REFERENCES

Armistead, S.E., Eglington, B.M., Pehrsson, S.J., 2021. PbIso: an R package and web app for calculating and plotting Pb isotope data. EarthArXiv; https://doi.org/10.31223/X56G84

Berendsen, P., Speczik, S., Wiszniewska, J., 1987. Sulphide geochemical studies of the stratiform tin deposits in the Stara Kamienica Chain (SW Poland). Archiwum Mineralogiczne, **42:** 31–42.

Berg, G., 1920. Zur Genesis und Systematik schlesischer Erzlagerstatten. Centralblatt für Mineralogie, Geologie und Paläontologie: 203–215.

Bobiński, W., 1997. The most important test results of the Gierczyn G-IV/19 and G-IV/26 boreholes (in Polish). Profile Głębokich Otworów Wiertniczych Państwowego Instytutu Geologicznego, **87:** 44–45.

Borkowska, M., Hameurt, J., Vidal, P., 1980. Origin and age of the Izera gneisses and Rumburk granites in the Western Sudetes. Acta Geologica Polonica, **30:** 122–146.

Cocherie, A., Legendre, O., Peucat, J.J., Koumelan, A.N., 1998. Geochronology of polygenetic monazites considered by in-situ microprobe Th-U-total lead determination: implications for lead behaviour in monazite. Geochimica et Cosmochimica Acta, **62:** 2475–2497; https://doi.org/10.1016/S0016-7037(98)00171-9

Cook, N.J., Dudek, K., 1994. Mineral chemistry and metamorphism of garnet-chlorite-mica schists associated with cassiterite-sulphide-mineralization from the Kamienica Range, Izera Mountains, S.W. Poland. Chemie der Erde, **54:** 1–32.

Cross, A., Jaireth, S., Rapp, R., Armstrong, R., 2011. Reconnaissance-style EPMA chemical U-Th–Pb dating of uraninite. Australian Journal of Earth Sciences. **58:** 675–683; https://doi.org/10.1080/08120099.2011.598190

Foltyn, K., Kozub-Budzyń, G.A., Lahaye, Y., Piestrzyński, A., Skirak, P., Zygo, W., Pieczonka, J., 2023. Mineralogy and in situ S and Pb isotope characteristics of ore minerals from polymetallic mineralization in the Gierczyn-Przecznica area, SW Poland. Geological Quarterly, **67**, 10; https://doi.org/10.7306/gq.1680

Franke, W., Żelaźniewicz, A., 2000. The eastern termination of the Variscides: terrane correlation and kinematic evolution. Geological Society Special Publications, **179:** 63–86; https://doi.org/10.1144/GSL.SP.2000.179.01.06

Griffin, B.J., Forbes, D., McNaughton, N.J., 2020. An Evaluation of Dating of Diagenetic Xenotime by Electron Microprobe. Microscopy and Microanalysis. **6:** 408–409; https://doi.org/10.1017/S143192760003453X

Harańczyk, C., Skiba, M., 1961. Gahnite from tin-bearing zone of Krobica-Gierczyn-Przecznica in Lower Silesia. Bulletin de L'Academie Polonaise des Sciences, Série des Sciences Géologiques et Géographiques, **9:** 149–154.

Jaskólski, S., 1960. Beitrag zur Kenntnis über die Herkunft der Zinnlagerstätten von Gierczyn (Giehren) im Iser-Gebirge, Niederschlesien. Neues Jahrbuch für Mineralogie-Abhandlungen, **94:** 181–190.

Jaskólski, S., 1963. Erwagungen über die Genese Zinnführender Schiefer im Isergebirge (Niederschlesien). Prace Geologiczne, **12:** 33–53.

Jaskólski, S., Mochnacka, K., 1959. The tin deposit in Gierczyn in the Izerskie Mountains in Lower Silesia and an attempt to explain its origin (in Polish). Archiwum Mineralogiczne, **22:** 17–106.

Jercinovic, M.J, Williams, M.I., 2005. Analytical perils (and progress) in electron microprobe trace element analysis applied to geochronology: Background acquisition, interferences, and beam irradiation effects. American Mineralogist, **90:** 526–546; https://doi.org/10.2138/am.2005.1422

Karwowski, Ł., Włodyka, R., 1981. Stannite in the cassiterite-sulphide deposits of the Izera Mts. (Sudetes). Acta Geologica Polonica, **31:** 41–47.

Konopásek, J., Anczkiewicz, R., Jerabek, P., Corfu, F., Žáčková, E., 2019. Chronology of the Saxothuringian subduction in the Eest Sudetes (Bohemian Massif, Czech Republic and Poland). Journal of the Geological Society, **176:** 492–504; https://doi.org/10.1144/jgs2018-173

Korytowski, A., Dörr, W., Żelaźniewicz, A., 1993. U-Pb dating of (meta)granitoids in the NW Sudetes (Poland) and their bearing on tectono-stratigraphic correlation. Terra Nova**, 5:** 331.

Kowalski, W., Karwowski, Ł., Śmietańska, I., Do Van, Phi., 1978. Ore mineralization of the Stara Kamienica schist belt in the Izera Mountains (in Polish). Prace Naukowe Uniwersytetu Śląskiego, **243**, Geol., **3:** 7–89.

Kozłowska-Koch, M., 1965. Granitogneisses of the Izera Foothills (in Polish). Archiwum Mineralogiczne, **25:** 123–260.

Kozłowski, A., 1978. Pneumatolytic and hydrothermal activity in the Karkonosze-Izera block. Acta Geologica Polonica, **28:** 171–222.

Kozłowski, K., 1974. Crystalline schists and leucogranites of the Stara Kamienica - Świeradów-Zdrój Belt (Western Sudetes) (in Polish with English summary). Geologica Sudetica, **9:** 7–98.

Kröner, A., Hegner, E., Hammer, J., Haase, J., Haase, G., Bielicki, K.H., Krauss, M., Eidam, J., 1994. Geochronology and Nd-Sm systematics of Lysatian granitoids: significance for the evolution of the Variscan orogen in east-central Europe. Geologische Rundschau, **83:** 357–376.

Kröner, A., Jaeckel, P., Hegner, E., Opletal, M., 2001. Single zircon ages and wholerock Nd isotopic systematics of early Palaeozoic granitoid gneisses from the Czech and Polish Sudetes (Jizerské hory, Krkonoše and Orlice-Sněžník Complex). International Journal of Earth Sciences, **90:** 304–324l; https://doi.org/10.1007/s005310000139

Kryza, R., Muszynski, A., Vielzeuf, D., 1990. Glaucophane-bearing assemblage overprinted by greenschist-facies metamorphism in the Variscan Kaczawa complex, Sudetes, Poland. Journal of Metamorphic Geology, **8:** 344–355.

Kryza, R., Mazur, S., Pin, C., 1995. Leszczyniec meta-igneous complex in the eastern part of the Karkonosze–Izera Block, Western Sudetes: trace element and Nd isotope study. Neues Jahrbuch für Mineralogie Abhandlungen, **170:** 59–74.

Kryza, R., Zalasiewicz, J., Mazur, S., Aleksandrowski, P., Sergeev, S., Larionov, A., 2007. Precambrian crustal contribution to the Variscan accretionary prism of the Kaczawa Mountains (Sudetes, SW Poland): evidence from SHRIMP dating of detrital zircons. International Journal of Earth Sciences, **96:** 1153–1162; https://doi.org/10.1007/s00531-006-0147-x

Kryza, R., Schaltegger, U., Oberc-Dziedzic, T., Pin, C., Ovtcharova, M., 2014. Geochronology of a composite granitoid pluton: a high-precision ID-TIMS U-Pb zircon study of the Variscan Karkonosze Granite (SW Poland). International Journal of Earth Sciences, **103:** 683–696; https://doi.org/10.1007/s00531-013-0995-0

Kucha, H., Mochnacka, K., 1998. Cassiterite micro inclusions in quartz and phyllosilicates from tin-bearing schists (Gierczyn, the Western Sudetes Mts., Poland) and their genetic significance. Mineralogica Polonica, **29:** 41–56.

Kusiak, M.A., 2007. CHIME – chemical method of mineral daring (in Polish with English summary). Przegląd Geologiczny, **55:** 383–389.

Machowiak, K., Armstrong, R., 2007. SHRIMP U–Pb zircon age from the Karkonosze granite. Mineralogia Polonica Special Papers, **31:** 193–196.

Majka, J., Mazur, S., Kosminska, K., Dudek, K., Klonowska, I., 2016. Pressure-temperature estimates of the blueschists from the Kopina Mt., northern Bohemian Massif, Poland – constraints on subduction of the Saxothuringian continental margin. European Journal of Mineralogy, **28:** 1047–1057; https://doi.org/10.1127/ejm/2016/0028-2601

Małek, R,. 2022. Mineralogical-geochemical study and genesis of a rare and accompanying elements occurrence within the tin-bearing deposit mineralization of the Stara Kamienica schist belt in the Sudetes (in Polish). Ph.D. Thesis. Narodowe Archiwum Geologiczne, PIG-PIB, Warszawa.

Małek, R., Mikulski, S.Z., Chmielewski, A., 2019. The geochemical-mineralogical characteristic of cassiterite-sulphide mineralization in the historic Saint John and Saint Leopold shafts in the Stara Kamienica shist belt (Western Sudetes) (in Polish with English summary). Przegląd Geologiczny, **67:** 914–924; https://doi.org/10.7306/2019.50

Mazur, S., Aleksandrowski, P., 2001. The Teplá(?)/Saxothuringian suture in the Karkonosze-Izera massif, Western Sudetes, Central European Variscides. International Journal of Earth Sciences, **90:** 341–360; https://doi.org/10.1007/s005310000146

Michniewicz, M., Bobiński W., Siemiątkowski J., 2006. Tin mineralization in the middle part of the Stara Kamienica schist belt (Western Sudetes) (in Polish with English summary). Prace Państwowego Instytutu Geologicznego, **186**.

Michniewicz, M., 1988. Tin-bearing ore zones in the Izera Mountains between Czerniawa and Krobica (in Polish). In: Metodyka rozpoznawania i dokumentowania złóż kopalin stałych. Rozpoznawanie i dokumentowanie złóż cyny. Materiały Seminarium: 5–20. Bierutowice. 10.06.1988. Wyd. AGH, Kraków.

Mikulski, S.Z., Kozłowski, A., Speczik, S., 2007. Fluid inclusion study of gold-bearing quartz-sulfide veins and cassiterite from the Czarnów As deposit ore (SW Poland). In: Digging Deeper (ed. J.A. Colin et al.) Volume: Proceedings of the Ninth Biennial SGA Meeting, Dublin 2007.

Mikulski, S.Z., Oszczepalski, S., Sadłowska, K., Chmielewski, A., Małek, R., 2018. The occurrence of associated and critical elements in the selected documented Zn-Pb, Cu-Ag, Fe-Ti-V, Mo-Cu-W, Sn, Au-As and Ni deposits in Poland (in Polish with English summary). Biuletyn Państwowego Instytutu Geologicznego, **472:** 21–52; https://doi.org/10.5604/01.3001.0012.7113

Mikulski, S.Z., Williams, I.S., Stein, H.J., Wierchowiec, J., 2020. Zircon U-Pb dating of magmatism and mineralizing hydrothermal activity in the Variscan Karkonosze Massif and its eastern metamorphic cover (SW Poland). Minerals, **10**, 787; https://doi.org/10.3390/min10090787

Mochnacka, K., Banaś M., 2000. Occurrence and genetic relationships of uranium and thorium mineralization in the Karkonosze Izera Block (the Sudety Mts, SW Poland). Annales Societatis Geologorum Poloniae, **70**: 137–150.

Montel, J.M., Foret, S., Veschambre, M., Nicollet, C., Provost, A., 1996. A fast, reliable, inexpensive, in-situ dating technique: Electron microporobe ages on monazite. Chemical Geology, **131:** 37–53; https://doi.org/10.1016/0009-2541(96)00024-1

Oberc, J., 1961. An outline of the geology ot the Karkonosze-Izera block (Studies on geology of the Sudetic Mountains). Zeszyty Naukowe Uniwersytetu Wrocławskiego, Nauka o Ziemi, 5, ser. B, **8:** 139–170.

Oberc, J., 1972. Sudetes and adjacent areas (in Polish). In: Budowa geologiczna Polski. T. IV, cz. 2, Wyd. Geol., Warszawa.

Oberc-Dziedzic, T., 1975. Gneiss enclaves in the Rumburk granite of the eastern part of the Izera Block (in Polish). Acta Universitatis Wratislaviensis, **247:** 165–210.

Oberc-Dziedzic, T., 1988. The development of gneisses and granites of the eastern part of the Izera crystalline in the light of texture studies (in Polish). Acta Universitatis Wratislaviensis, **997**: 1–184.

Oliver, G.J.H., Corfu, F., Krogh, T.E., 1993. U-Pb ages from SW Poland: Evidence for Caledonian suture zone between Baltica and Gondwana. Journal of the Geological Society, **150**: 355–369.

Ozha, M.K., Pal, D.P., Mishra, B., Desapati, T., Shaji, T.S., 2017. Geochemistry and chemical dating of uraninite in the Samarkiya area, central Rajasthan, northwestern India – Implication for geochemical and temporal evolution of uranium mineralization. Ore Geology Reviews, **88:** 23–42; https://doi.org/10.1016/j.oregeorev.2017.04.010

Parrish, R.R., 1990. U-Pb dating of monazite and its application to geological problems. Canadian Journal of Earth Sciences, **27:** 1431–1450; https://doi.org/10.1139/e90-152

Pieczonka, J., Nguyen, C.D., Piestrzyński, A., Le, P.K., 2019. Timing of ore mineralization using ore mineralogy and U-Pb dating, Iron Oxide Copper Gold Sin Quyen deposit, North Vietnam. Geological Quarterly, **63** (4): 861–874; https://doi.org/10.7306/gq.1507

Piestrzyński, A., Mochnacka, K., Mayer, W., Kucha, H,. 1992. Native gold (electrum), Fe-Co-Ni arsenides and sulphoarsenides in the mica schists from Przecznica, The Kamienica Range, SW Poland. Mineralogica Polonica, **23:** 27–43.

Pyle, J.M., Spear, F.S., Wark, D.A. Daniel, C.G., Storm, I.C., 2005. Contribution to precision and accuracy of monazite microprobe ages. American Mineralogist, **88:** 547–577; https://doi.org/10.2138/am.2005.1340

Siemiątkowski, J., 1986. Views on the genesis of the tin deposits of the Kamineneckie Range schists (in Polish). Kwartalnik Geologiczny, **30** (1): 126.

Siemiątkowski, J., 1988. Structures and textures of cassiterite-sulphide mineralization of the western part of the Kamieniec range in the Izera Mountains (in Polish). Kwartalnik Geologiczny, **32** (3): 220–221.

Siemiątkowski, J., 1989. Laminated textures of cassiterites from mica schists near Czerniawa Zdrój in the Izera Mountains (in Polish). Przegląd Geologiczny, **37**: 430–432.

Siemiątkowski, J., 1991. Structures and textures of cassiterite in mineralized metamorphic schists of the Kamieniec range of the Izera Mountains and their genetic significance (in Polish with English summary). Biuletyn Państwowego Instytutu Geologicznego, **367:** 49–60.

Smulikowski, W., 1995. Evidence of glaucophane-schist facies metamorphism in the East Karkonosze complex, West Sudetes, Poland. Geologische Rundschau, **84:** 720–737.

Smulikowski, W., 1972. Petrographic and structural problems of the northern cover of the Karkonosze granite (in Polish with English summary). Geologica Sudetica, **6:** 97–188.

Speczik, S., Wiszniewska, J., 1984. Some comments about stratiform tin deposits in the Stara Kamienica Chain (southwestern Poland). Mineralium Deposita, **19:** 171–175.

Stacey, J.T., Kramers, J.D., 1975. Approximation of terrestrial lead isotope evolution by a two-stage model. Earth and Planetary Science Letters, **26:** 207–221.

Suzuki, K., Adachi, M., 1991a. Precambrian provenance and Silurian metamorphism of the Tsubonosawa paragneiss in the South Kitakami terrane, Northeast Japan, revealed by the chemical Th-U-total Pb isochron ages of monazite, zircon and xenotime. Geochemical Journal, **25:** 357–376.

Suzuki, K., Adachi, M., 1991b. The chemical Th–U–total Pb isochron ages of zircon and monazite from the gray granite of the Hida Terrane, Japan. The Journal of Earth and Planetary Sciences, **38:** 11–38.

Suzuki, K., Dunkley, D.J., 2015. Uranium-lead, chemical isochron U-Pb method (CHIME). Encyclopedia of Scientific Dating Methods. (eds. W.J. Rink and J.W. Thompson): 863–869. Springer, Dordrecht; https://doi.org/10.1007/978-94-007-6326-5_200-1

Suzuki, K., Kato, T., 2008. CHIME dating of monazite, xenotime, zircon and polycrase: Protocol, pitfalls and chemical criterion of possibly discordant age data. Gondwana Research. **14:** 569–586; https://doi.org/10.1016/j.gr.2008.01.005

Suzuki, K., Adachi, M., Tanaka, T., 1991. Middle Precambrian provenance of Jurassic sandstone in the Mino Terrane, central Japan: Th–U–total Pb evidence from an electron microprobe monazite study. Sedimentary Geology, **75:** 141–147; https://doi.org/ 10.1016/0037-0738(91)90055-I

Szałamacha, M., 1967. About tin mineralization in the eastern part of the Kamieniec range in the Izera Mountains (in Polish with English summary). Przegląd Geologiczny, **15:** 281–284.

Szałamacha, M., 1976. On the origin of cassiterite mineralization in the metamorphic schists of the Karkonosze-Góry Izerskie (Mts.) Block, the Sudetes. In: The current metallogenic problems of Central Europe (ed. J. Fedak): 343–349. Wyd. Geol., Warszawa.

Szałamacha, M., Szałamacha, J., 1964. The problem of northern contact of the mica schists of the Kamieniec Range with the Izera gneiss (in Polish with English summary). Przegląd Geologiczny, **12:** 329–331.

Williams, M.L., Jercinovic, M.J., Hetherington, C.L., 2007. Microprobe monazite geochronology: understanding geologic processes by integrating composition and chronology. Annual Review of Earth and Planetary Sciences. **35:** 137–175; https://doi.org/10.1146/annurev.earth.35.031306.140228

Winchester, J.A., Floyd, P.A., Chocyk, M., Horbowy, K., Kozdrój, W., 1995. Geochemistry and tectonic environment of Ordovician meta-igneous rocks in the Rudawy Janowickie Complex, SW Poland. Journal of the Geological Society, **152:** 105–115.

Winchester, J.A., Patočka, F., Kachlík, V., Melzer, M., Nawakowski, C., Crowley, Q.G., Floyd, P.A., 2003. Geochemical discrimination of metasedimentary sequences in the Karkonose–Jizera Terrane (West Sudetes, Bohemian Massif): paleotectonic and stratigraphic constraints. Geologica Carpathica, **54**: 267–280.

Wiszniewska, J., 1983. Problem of genesis of tin mineralization of the Izera schists in Kamienickie Range. Archiwum Mineralogiczne, **38**: 45–55.

Wiszniewska, J., 1984. The genesis of mineralization of the Izera shales from the Kamieniec Range (in Polish with English summary). Archiwum Mineralogiczne, **40:** 115–187.

Zygo, W., Foltyn, K., Thomasen, T.B., Heredia, B.D., Piestrzyński, A., 2023. Preliminary results of U-Pb dating and trace element analysis of cassiterites from the Western Sudetes, SW Poland. In: Proceedings of the 17th SGA Biennial Meeting, 28 August – 1 September 2023, **1**: 331–335.

Żaba, J., 1984. Genesis and metamorphic evolution of gneisses and granitoids of the Izerski Stóg Massif, Western Sudetes) (in Polish with English summary). Geologica Sudetica, **19**: 89–190.

Žáčková, E., Konopásek, J., Jeřábek, P., Finger, F., Košler, J., 2010. Early Carboniferous blueschist facies metamorphism in metapelites of the West Sudetes (Northern Saxothuringian Domain, Bohemian Massif). Journal of Metamorphic Geology, **28:** 361–379; https://doi.org/10.1111/j.1525-1314.2010.00869.x

Žáčková, E., Konopásek, J., Košler, J., Jeřábek, P., 2012. Detrital zircon populations in quartzites of the Krkonoše-Jizera Massif: implications for pre-collisional history of the Saxothuringian Domain in the Bohemian Massif. Geological Magazine, **149:** 443–458; https://doi.org/10.1017/S0016756811000744

APPENDIX 1

EMPA analysis conditions

Signal(s) Used: Si Kα, Hf Mα, Al Kα, Y Lα, Sr Lα, Lu Lβ, Tm Lβ, Ho Lβ, Yb Lα, Er Lα, Dy Lα, Fe Kα, Tb Lα, Gd Lα, Eu Lα, Sm Lα, As Lβ, Nd Lβ, P Kα, Zr Lα, S Kα, K Kα, Ca Kα, Th Mα, U Mβ, Pb Mβ.

Column Conditions: 15keV, 200nA.

Analysis Parameters:

Elements	Xtal	Position	Bg+	Bg-	Slope	Bias	Gain	Dtime	Blin	Wind
Si Ka	TAP	27740		1400	1,1	1312	3056	3	560	
Hf Ma	TAP	29320	-400	500		1300	2977	3	1586	3414
Al Ka	TAP	32459	-2400	2800		1313	3057	3	560	
Y La	LPET	73640	-1200	1200		1848	1014	3	560	
Sr La	LPET	78415		1000	1	1822	595	3	459	1790
Lu Lb	LLIF	35340	-800	800		1829	425	3	1844	1968
Tm Lb	LLIF	38010	-900	600		1825	425	3	1679	1906
Ho Lb	LLIF	40870	-1000	1150		1820	425	3	1531	1830
Yb La	LLIF	41475	-1600	1600		1827	423	3	560	
Er La	LLIF	44290	-600	600		1820	425	3	1376	1762
Dy La	LLIF	47390	-800	1200		1839	442	3	1258	1704
Fe Ka	LLIF	48088	-1500	1900		1821	426	3	560	
Tb La	LLIF	49050	-400	950		1820	425	3	1201	1674
Gd La	LLIF	50800	-800	800		1850	415	3	1145	1644
Eu La	LLIF	52655	-600	500		1820	425	3	1092	1614
Sm La	LLIF	54620	-600	500		1820	425	3	1036	1588
As Lb	TAP	36615	-1000	2000		1314	3108	3	1097	3266
Nd Lb	LLIF	53800	-400	400		1820	425	3	1058	1600
P Ka	LPET	70360	-2500	1500		1313	1033	3	526	1924
Zr La	LPET	69390	-1800	2600		1306	1059	3	530	1948
S Ka	LPET	61386		1600	1	1310	1037	3	527	2205
K Ka	LPET	42769		800	1	1313	1012	3	1014	2648
Ca Ka	LPET	38388	-700	800		1311	1042	3	560	
Th Ma	LPET	47285	-1200	800		1306	1059	3	858	2512
U Mb	LPET	42400	-1200	800		1847	1006	3	1027	2660
Pb Mb	LPET	57975	-1050	1300		1847	1006	3	588	2272

Used standard composition:

- Wollastonite = O: 41.17%, Na: 0.01%, Mg: 0.01%, Si: 23.99%, Ca: 34.17%, Ti: 0.01%, Mn: 0.49%, Fe: 0.15%
- 47-ZrO_2 Zirconia = O: 24.91%, Y: 14.37%, Zr: 59.17%, Hf: 1.51%
- Orthoclase = O: 46.28%, Na: 1.01%, Al: 9.82%, Si: 30.43%, K: 12.19%, Ca: 0.01%, Ti: 0.01%, Mn: 0.01%, Fe: 0.02%, Sr: 0.04%, Ba: 0.13%
- Xenotime = O: 31.7%, Si: 0.04%, P: 15.28%, Y: 33.62%, Nd: 0.14%, Sm: 0.67%, Eu: 0.43%, Gd: 3.8%, Tb: 0.83%, Dy: 6.4%, Er: 3.42%, Yb: 3.42%, Th: 0.14%
- $SrTiO_3$ = Sr: 47.7442%, Ti: 26.1007%, O: 26.1551%
- 23_Lu-glass = O: 42.42%, Al: 6.75%, Si: 25.5%, Ca: 14.78%, Lu: 10.55%
- 21_Tm-glass = O: 42.55%, Al: 6.75%, Si: 25.5%, Ca: 14.78%, Tm: 10.42%
- $HoPO_4$ = Ho: 63.4582%, P: 11.9174%, O: 24.6244%
- $YbPO_4$ = Yb: 64.5639%, P: 11.5568%, O: 23.8793%

- $ErPO_4$ = Er: 63.7828%, P: 11.8115%, O: 24.4056%
- $DyPO_4$ = Dy : 63.1133%, P : 12.0299%, O: 24.8568%
- 34-Olivine = O: 43.89%, Mg: 30.42%, Si: 19.44%, Mn: 0.08%, Fe: 5.87%, Ni: 0.3%
- 17_Tb_Glass = O: 42.85%, Al: 6.75%, Si: 25.5%, Ca: 14.78%, Tb: 10.12%
- $GdPO_4$ = Gd: 62.3455%, P: 12.2803%, O: 25.3742%
- $EuPO_4$ = Eu: 61.5388%, P: 12.5434%, O: 25.9178%
- $SmPO_4$ = Sm: 61.2943%, P: 12.6231%, O: 26.0826%
- Arsenopyrite FeAsS = Fe: 34.44%, As: 44.83%, S: 20.73%
- $NdPO_4$ = Nd: 60.2976%, P: 12.9482%, O: 26.7542%
- 04-Apatite = O: 38.07%, F: 3.77%, P: 18.42%, Ca: 39.74%
- $ZrSiO_4$ (2) = O: 34.75%, Si: 15.24%, Zr: 49.1%, Hf: 0.91%
- $BaSO_4$ = O: 27.42%, S: 13.74%, Ba: 58.84%
- 2_Orthoclase = O: 46.31%, Na: 1.01%, Al: 9.82%, Si: 30.45%, K: 12.2%, Ca: 0.01%, Mn: 0.01%, Fe: 0.02%, Sr: 0.04%, Ba: 0.13%
- 25_Th_Glass_2 = Al: 7.3826%, Si: 27.1865%, Ca: 15.7244%, Th: 5.1736%, O: 44.533%
- 26_U_Glass_2 = O: 45.002%, Al: 7.4386%, Si: 27.5911%, Ca: 16.1066%, U: 3.8618%
- 28_Crocoite = O: 19.8%, Cr: 16.09%, Pb: 64.11%

<u>Beam Size:</u> 1 µm.

<u>Used dating standard</u>: xenotime from Iveland [Nor], age = +/- 900 Ma

	Weight%														
Point#	Si	Hf	Y	Sr	Lu	Tm	Ho	Yb	Er	Dy	Tb	Gd	Eu	Sm	Nd
1	1,595	0,031	31,341	0,006	1,063	0,293	0,577	4,639	2,457	2,616	0,24	1,183	0,029	0,423	0,231
2	1,58	0,011	31,241	0,002	0,939	0,389	0,592	4,802	2,524	2,594	0,243	1,217	0,017	0,382	0,245
3	1,573	0,025	31,482	0	0,729	0,285	0,641	4,614	2,485	2,643	0,207	1,197	0,022	0,401	0,219
4	1,585	0,04	31,129	0,006	0,943	0,309	0,466	4,631	2,547	2,603	0,268	1,182	0,004	0,395	0,303
5	1,547	0,014	31,66	0,014	0,947	0,288	0,623	4,772	2,565	2,636	0,268	1,242	0,008	0,378	0,225
6	1,543	0,035	31,781	0,018	0,93	0,213	0,655	4,665	2,493	2,616	0,253	1,223	0	0,4	0,322
avr. det. lim. [wt.%]	152	253	447,6	390	2761	1499,6	2018,2	1089,8	922,2	1022	796	788,6	604,5	729,4	1263

	Weight%											
Point#	P	Zr	S	K	Ca	Th	U	Pb	O	Total	Age (Ma)	Age err
1	13,256	0,461	0,103	0,006	0,015	5,91	1,465	0,443	30,599	98,983	899	52
2	13,275	0,461	0,109	0,014	0,019	5,943	1,483	0,448	30,614	99,147	903	52
3	13,171	0,447	0,11	0,014	0,019	5,99	1,502	0,455	30,474	98,708	907	52
4	13,122	0,453	0,1	0,011	0,02	6,168	1,501	0,467	30,392	98,653	915	52
5	13,21	0,446	0,111	0,006	0,011	5,922	1,486	0,45	30,598	99,436	906	52
6	13,167	0,421	0,102	0,006	0,007	6,088	1,487	0,461	30,564	99,45	915	52
avr. det. lim. [wt.%]	102,6	316,2	181,6	129,4	141,6	120	134,8	124,6				

avr. det. lim. - average detection limit.

APPENDIX 2

Summary of EMPA results for uraninites along with detection limits

	Oxide [wt.%]																Total	Age (Ma)
	UO_2	**PbO**	**FeO**	**ThO_2**	**Y_2O_3**	**K_2O**	**Gd_2O_3**	**SiO_2**	**Dy_2O_3**	**Sm_2O_3**	**CaO**	**Nd_2O_3**	**Eu_2O_3**	**Lu_2O_3**	**Ce_2O_3**	**P_2O_5**		
uraninite	92.335	4.452	0.235	1.605	0.097	Bdl.	Na.	0.086	Na.	Na.	Bdl.	0.154	Na.	Na.	0.068	0.011	99.106	**350 ± 15**
	93.621	4.5	1.28	0.001	0.222	Bdl.	Na.	0.08	Na.	Na.	Bdl.	0.05	Na.	Na.	Bdl.	0.002	99.82	**351 ± 15**
	94.123	4.504	0.755	Bdl.	0.417	Bdl.	Na.	0.087	Na.	Na.	0.017	Bdl.	Na.	Na.	0.032	Bdl.	99.995	**349 ± 15**
	91.75	4.399	1.634	Bdl.	0.973	Bdl.	Na.	0.133	Na.	Na.	Bdl.	0.086	Na.	Na.	0.101	0.019	99.249	**350 ± 15**
	83.885	3.422	1.757	0.229	0.327	0.293	0.29	0.628	0.185	0.174	Bdl.	0.013	0.033	0.025	Na.	0.006	91.318	**299 ± 7**
	88.696	4.468	1.595	0.074	0.286	0.281	0.279	0.463	0.19	0.124	Bdl.	Bdl.	0.078	0.041	Na.	0.002	96.665	**367 ± 8**
	82.591	3.466	3.288	0.1	0.267	0.303	0.283	0.114	0.193	0.143	Bdl.	0.1	0.053	0.157	Na.	Bdl.	91.235	**307 ± 7**
	85.189	3.483	2.912	0.737	0.469	0.273	0.216	0.257	0.133	0.13	Bdl.	0.098	0.063	Bdl.	Na.	0.003	94.222	**299 ± 7**
	88.116	4.396	2.407	0.024	0.037	0.299	0.09	0.167	Bdl.	0.15	Bdl.	0.141	0.097	0.014	Na.	0.003	96.105	**363 ± 8**
	87.75	4.393	0.418	Bdl.	0.251	0.271	0.341	0.028	0.241	0.138	Bdl.	Bdl.	0.043	0.042	Na.	Bdl.	93.996	**365 ± 8**
	87.876	4.362	0.414	Bdl.	0.254	0.269	0.295	0.574	0.204	0.203	Bdl.	Bdl.	0.094	0.131	Na.	0.01	94.738	**362 ± 8**
avr. [wt.%]	88.721	4.168	1.518	0.396	0.327	0.284	0.256	0.238	0.191	0.152	0.017	0.092	0.066	0.068	0.067	0.007	96.041	
element	**U**	**Pb**	**Fe**	**Th**	**Y**	**K**	**Gd**	**Si**	**Dy**	**Sm**	**Ca**	**Nd**	**Eu**	**Lu**	**Ce**	**P**		
avr. det. lim [ppm]	349	132	531	120	464	154	915	201	1184	867	201	1499	722	3154	1559	95		

Bdl. – below detection limit; Na. – not analyzed; avr. – average (arithmetic); avr. det. lim. – average detection limit.